Ten Factors About Standing Supports That Might Surprise You

Timothy Batchler, Mechanical Engineer
Ground Control Branch
NIOSH, Office of Mine Safety and Health Research
Pittsburgh, PA

ABSTRACT

Standing roof supports help to provide a stable working environment in coal mine gateroads. NIOSH participates in the development of these support systems by conducting full-scale tests in their Mine Roof Simulator. These tests have established the performance characteristics of every coal mine support system currently in use in the United States. Through these tests, mine operators and regulatory officials have acquired a fundamental understanding of the various types of support performance that guides the assessment and use of these support systems. However, some little known factors that influence support behavior can lead to misconceptions and, perhaps, a poor assessment of support behavior at times. This paper highlights several of these factors and discusses their significance. The paper also examines a current longwall tailgate support and discusses the inefficiency with this approach. Finally, the NIOSH Mine Roof Simulator (MRS) is the world's most powerful load frame built specifically to test full-scale roof supports, including longwall shields. are addressed in this paper to provide a more in-depth assessment of the limitations of the MRS and what the MRS testing protocol is designed to do.

INTRODUCTION

Over the years, considerable research has been conducted to develop standing support technologies and to evaluate their performance characteristics. The load and displacement characteristics of the standing supports have been determined from full-scale testing conducted using the National Institute for Occupational Safety and Health (NIOSH) Mine Roof Simulator (MRS) (Barczak and Tadolini, 2008) located in Bruceton, PA. Performance traits, installation patterns, and ground responses are observed in various geological and mining conditions and are evaluated to determine the support performance in the field (Dolinar, 2010; Campoli, 2015; Zhang et al., 2012). Despite widespread use of standing supports, not every aspect of their performance and resulting ground support capability are always well understood. This paper discusses 10 factors, several of which are surprising, that impact standing support performance.

TEN FACTORS THAT INFLUENCE SUPPORT BEHAVIOR

Topics included in the 10 factors are as follows: (1) the contribution of support components, (2) extreme support performance capabilities, and (3) putting the MRS capability in perspective regarding ground behavior. The ultimate goal is to ensure safe applications of these innovative support systems.

FACTOR 1: Independently, the individual components do not add up to the full support capacity of the CAN support.

The CAN support is a cylindrical steel shell encompassing an aerated concrete core (Figure 1). Tests were conducted separately on each component of the CAN to evaluate the contribution of the exterior steel shell and aerated concrete core to the overall support capacity. The aerated concrete core component was tested by removing the exterior steel shell from a 36-inch-diameter CAN. However, the steel shell test was conducted on a 24-inch-diameter shell because another 36-inch-diameter shell was not available. The capacity of the 36-inch-diameter shell was then computed under the assumption that the shell would fail at the same stress measured in the 24-inch-diameter shell test. Full-scale load tests were also conducted on a standard 24- and 36-inch-diameter CAN support.

As seen in Figure 2, the CAN support provides more load capacity than the sum of the aerated concrete core and steel shell components. These test results demonstrate that the individual components must work together to provide the total performance capacity of the support. In addition, the post-yield behavior for the individual components is different than that of the complete CAN support. The CAN support sustains a steady residual load following yielding while both of the individual components shed load after yielding.

FACTOR 2: Without confinement of the fill material, the CAN and pumpable roof supports would not provide adequate support capability, but the interaction of the fill material is different in each support.

Pumpable and CAN supports are used to control the stability of the immediate roof in tailgates. The cementitious material

Figure 1. Image of a CAN support at NIOSH's Mine Roof Simulator (MRS) facility.

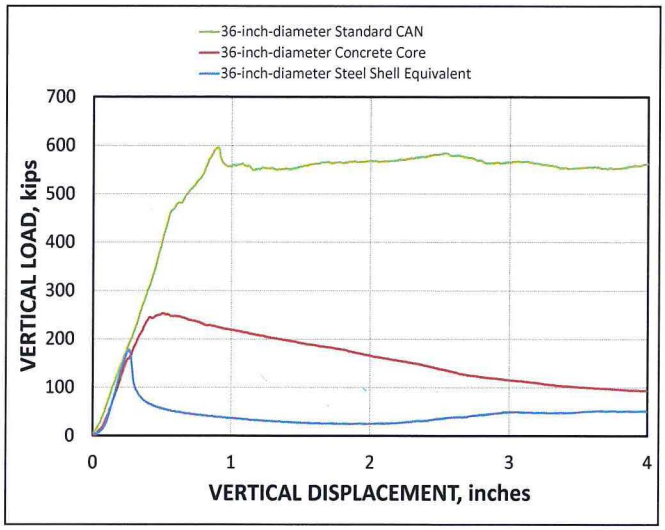

Figure 2. Load-displacement performance comparison of a complete CAN support and its individual components.

properties of each support play a significant role in the performance of the support. Figure 3 shows the performance characteristics of each support type with and without confinement. The CAN support uses an aerated concrete, which is placed inside a steel shell. The loading characteristics of the CAN support is an initial stiff elastic response that causes a rapid build-up of load followed by a slight strain-hardening yielding phase. When confined by the steel shell, the aerated concrete crushes into a powder consistently filling the voids and maintains a steady yielding performance. For the unconfined CAN support, initially, there is a stiff elastic response, but after the peak load capacity is reached, the support exhibits a gradual load shedding performance profile. For this example, the aerated concrete accounts for 44% of the peak load capacity of the CAN support.

A pumpable support is formed when a two-part, fast-setting grout is pumped into a containment bag, which acts as a form to fill the support and provides confinement to the grout during peak and residual loading. When the compressive strength of the grout is exceeded, the grout will fracture, and the support will abruptly shed

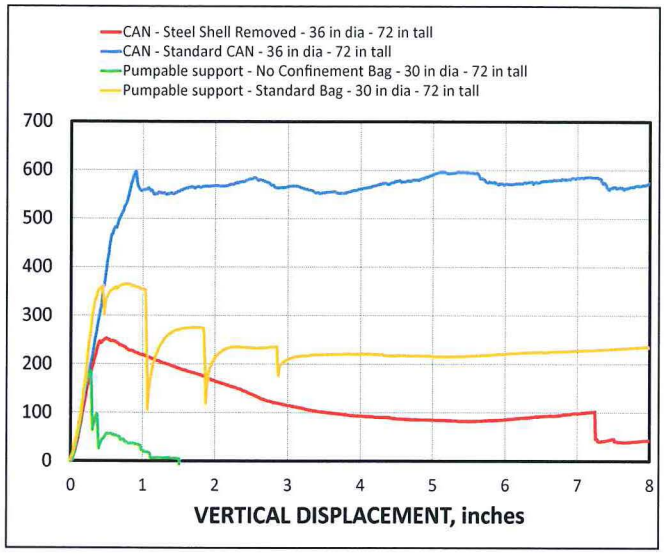

Figure 3. Pumpable and CAN load-displacement curve results for both confined and unconfined supports.

its load capacity. Figure 4 shows that the unconfined pumpable material sheds its peak load capacity with little residual load. For this example, the unconfined material accounts for 51% of the load capacity for the pumpable support. When the standard pumpable support starts to fail, the load capacity is transferred from a grout-only capacity to the confinement of the grout in the containment bag. The containment bag is then able to retain the grout core to provide sufficient deformability (yield). While confinement is important to both support systems, the fill material in the CAN aids in the stability of the shell, whereas the pumpable fill material does not contribute to the stability of the bag.

FACTOR 3: Splits in the body of a propsetter do not affect the peak load capacity or stiffness of the prop.

The Propsetter is a timber post engineered to provide controlled yielding without buckling of the prop. Wedges are cut into the bottom section of the prop, creating a tapered solid core that progressively crushes during load applications. Steel bands are also added to provide confinement to the central core during crushing. As with most timber supports, splits can occur on the Propsetter (Figure 4). Splits occur when the equilibrium moisture content of the environment (mine or storage area) is lower than the moisture content of the wood in the Propsetter. When this happens, the wood starts to lose moisture. Since water moves through the end grain much faster than through the sides, the ends begin drying quickly and tend to shrink, creating tensile stresses. If the tensile stresses exceed the strength of the wood, a split will occur (Figure 4). However, splits in a Propsetter do not affect the peak load capacity of the support (Figure 5). As seen from tests conducted in the MRS, splits in the Propsetter did not affect the buckling strength of the support. This behavior can be validated by calculating the buckling strength of a timber post using Equations 1 and 2 (Hicks, 2010).

$$Pcr = \frac{3.619 * A * E}{\left(\frac{L}{r}\right)^2} \qquad (1)$$

Figure 4. Images of a Propsetter with severe splits.

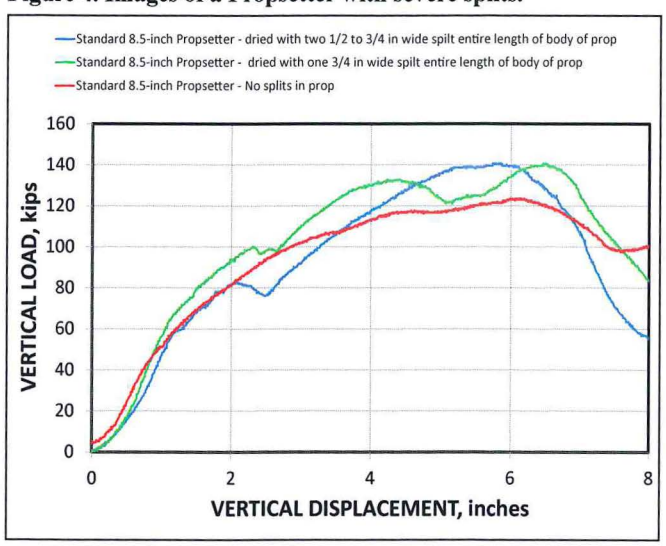

Figure 5. Load-Displacement performance comparison of Propsetters with severe splits in the support.

$$r = \sqrt{\frac{I}{A}} \qquad (2)$$

where

Pcr = critical or maximum axial load on the timber column just before it begins to buckle

E = modulus of elasticity of the material, lb/in^2

A = column cross-sectional area, in^2

L = effective length of the column, in

r = radius of gyration of the column, in

I = least moment of inertia of the column cross-sectional area A, in^4

Using an 8.5-inch-diameter Propsetter at a support height of 84 inches as an example, the calculated buckling load of the support is 208 kips. In a worst-case scenario in which the 8.5-inch-diameter Propsetter would completely split into two pieces, Equations 1 and 2 determine that the buckling force needed to fail each half section of the support is 104 kips. Similarly, the slenderness ratio (L/r), which is the measure of the flexibility of a column under load, is unaffected by splits with both the unsplit Propsetter and the split (in half) Propsetter, each having a slenderness ratio of 39.5. A standard timber post with a slenderness ratio ranging from 18–50 is controlled by the elastic stability limit and indicates that buckling failure will likely occur. However, the Propsetter, even with the splits, is able to reach the designed peak load capacity and not buckle because the yielding (failure) mechanism is controlled by the bottom wedge section and not the main post (full diameter) body.

FACTOR 4: Roof channel significantly improves the effectiveness of roof screen.

Load-displacement tests were conducted on wire roof screens in a specially designed frame for the MRS. These tests were designed to simulate loading conditions caused by the bagging of fallen roof rock that is captured by the screen. Figure 6 shows an 8-ft by 12-ft section of roof screen mounted to the test fixture in the MRS. The test fixture is designed to accommodate the standard 4-ft by 4-ft roof bolt spacing for anchoring the screen. Two 5-inch-wide metal roof channels were anchored on 4-ft spacing across the screen in the test configuration shown in Figure 6.

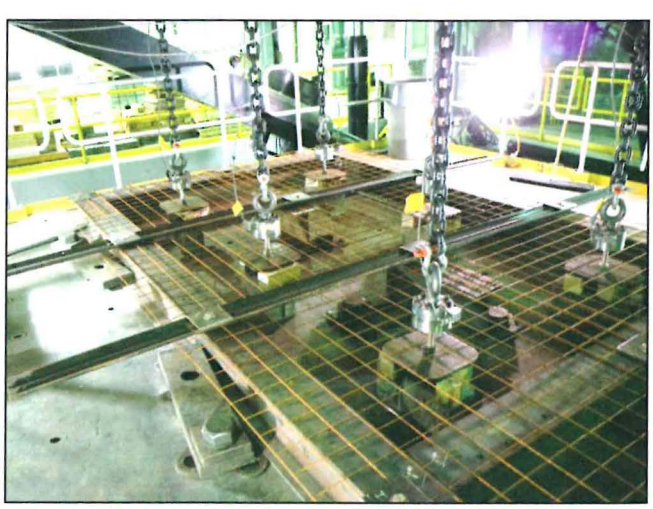

Figure 6. Test frame setup used to test screen material.

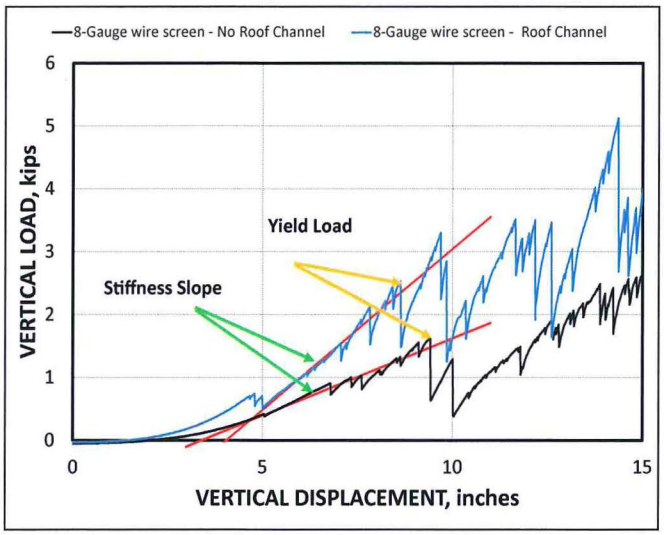

Figure 7. Load-displacement curves comparing screen with and without roof channel.

Figure 8. Example of an 18-layer Hercules crib.

The MRS test results demonstrate that roof channels can improve the effectiveness of roof screen by increasing the load capacity and system stiffness. For example, the load-displacement graphs for a #8 gauge wire screen tested with and without a roof channel are shown in Figure 7. The yield load is the load just prior to a significant drop in load. In this case, Figure 7 shows a 55% increase in the yield load capacity of the screen when a roof channel is used. The system stiffness is determined as the slope of a line from the point when the screen begins to significantly resist load to the yield load. The roof channel, shown in Figure 7, increases in system stiffness by 108% for this test.

FACTOR 5: A Hercules crib can support more load than a modern longwall shield.

Operating longwall faces generally use shield supports to provide ground control. The longwall shield must be able to resist large force reactions caused by the main roof and overburden weighting. Modern longwall shields have an average capacity of 1,019 tons, with the highest capacity shield rated at 1,327 tons (Fiscor, 2016). Wood cribs are generally used as secondary support in longwall tailgates. Conventional 4-point wood cribs have a rated (yield) capacity of about 50 tons. However, engineered timber supports can have significantly higher capacity. In fact, the Hercules crib (Figure 8) can be designed to provide a load capacity higher than that of a modern longwall shield. The Hercules crib is constructed from preformed mats that are composed of short blocks of wood and sandwiched between timber slabs. This design feature combines end-grain timber loading with cross-grain timber loading to combine the characteristics of a wood post (high stiffness) and conventional wood crib (large yield) into a single support. A 30-inch x 30-inch white oak Hercules crib is capable of carrying 1,488 tons at 21 inches of convergence compared to the largest longwall shield currently used in the United States with a rated roof support yield of 1,327 tons (Fiscor, 2016).

FACTOR 6: The CAN support has the extreme capacity to withstand horizontal movement.

The CAN support is a thin-walled steel shell that provides confinement to aerated concrete fill material, which crushes to a powder-like consistency when loaded. The support is extremely stable and is not significantly affected by asymmetric loading or stress concentrations. The CAN support is capable of withstanding large degrees of horizontal top-to-bottom (simulating roof-to-floor) movement without shedding load or losing stability. Figure 9 shows test results from two 24-inch-diameter CANs that were tested at the MRS. Load orientation varied from a pure vertical displacement to simultaneous applications of vertical and horizontal displacement at a ratio of 1 to 1. Based on these observations, the CAN support can perform well in high horizontal displacement situations. Figure

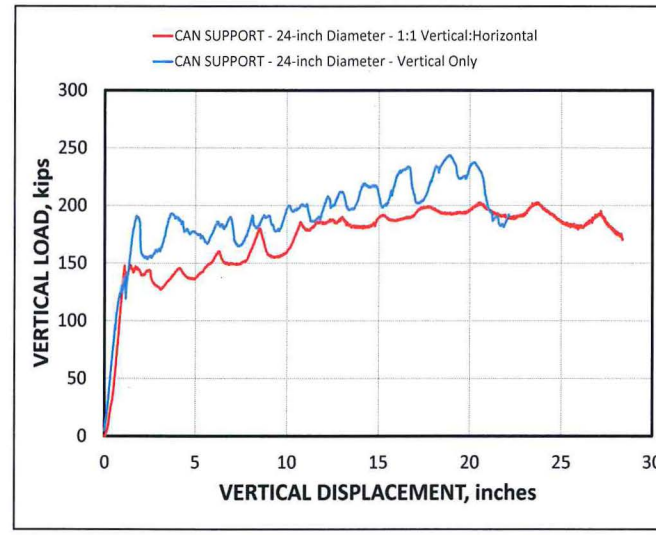

Figure 9. Load-displacement performance data for vertical and 1:1 vertical:horizontal CAN support.

Figure 10. Example of pre- and post-yield behavior of a CAN support after 28-inches of 1:1 vertical:horizontal displacement.

10 shows the 24-inch-diameter CAN support after 28 inches of vertical and horizontal displacement. As seen in the photo, there are no signs of failure or instability.

FACTOR 7: Some pumpable support material will decompose when exposed to air.

Since all pumpable supports are visually similar and installed fundamentally in the same manner, there is a tendency to believe that they all have similar material properties. One interesting difference is that some types of Portland-cement-based pumpable support material severely decomposes when exposed to air. Material grout samples were taken from a pumpable support after testing in the MRS (Figure 11). When exposed to air for one day, the grout samples began to dry out and started to show signs of decomposition. As seen in Figure 12, when left exposed for 12 days in a lab setting, the material is highly decomposed. However, the performance of the pumpable support did not appear to be compromised, which occurs when there is no damage to the containment bag. Because the support material was not exposed to the air, no decomposition of the pumpable material was indicated.

FACTOR 8: Timber orientation can significantly affect wood crib support capacity and stability.

Strength, stiffness, and stability are the criteria that must be considered for an acceptable support design. However, changing the timber orientation can dramatically change the performance characteristics of a conventional wood crib. For example, Figure 13 compares the performance of 4-point wood cribs constructed from 5-inch x7-inch x 36-inch timber, one with the wide (7-inch) side of the timber placed horizontally to establish the timber contact and the other with the narrow (5-inch) side of the timber oriented to establish the interlayer timber contact. Test results show that the crib strength, which is determined by its capacity to support load, increased for the wider timber contact orientation. In this example, the load capacity at 8-inches displacement for the 5-inch-

Figure 11. Example of pumpable material sample taken right after testing at the MRS.

Figure 12. Pumpable material sample, 12 days after testing at the MRS, when left exposed to air in the lab setting.

wide orientation to establish the timber interlayer contact was 139 kips, which increased by 71 percent to 238 kips for the 7-inch-wide timber interlayer contact orientation. The crib stiffness is determined by computing the slope of the load-displacement curve during the initial (linearly elastic) response of the support. The initial stiffness with the 5-inch-wide timber contact orientation was 52.9 kips/in, and the stiffness with the 7-inch-wide timber contact orientation was 123.3 kips/in. Thus, rotating the timber resulted in a 133% increase in the crib stiffness. Stability is a measure of the capability of a structure to maintain equilibrium without sudden or severe loss of load capacity. The 5-inch-wide timber orientation did not remain as stable as the 7-inch-wide timber orientation and experienced a reduction in load capacity at 9 inches of displacement as the crib started to buckle (Figure 14).

FACTOR 9: Only the abutment zone needs the additional support provided by a standing support system.

The universal practice for ground control in longwall tailgates is to support the entire tailgate with some form of standing support.

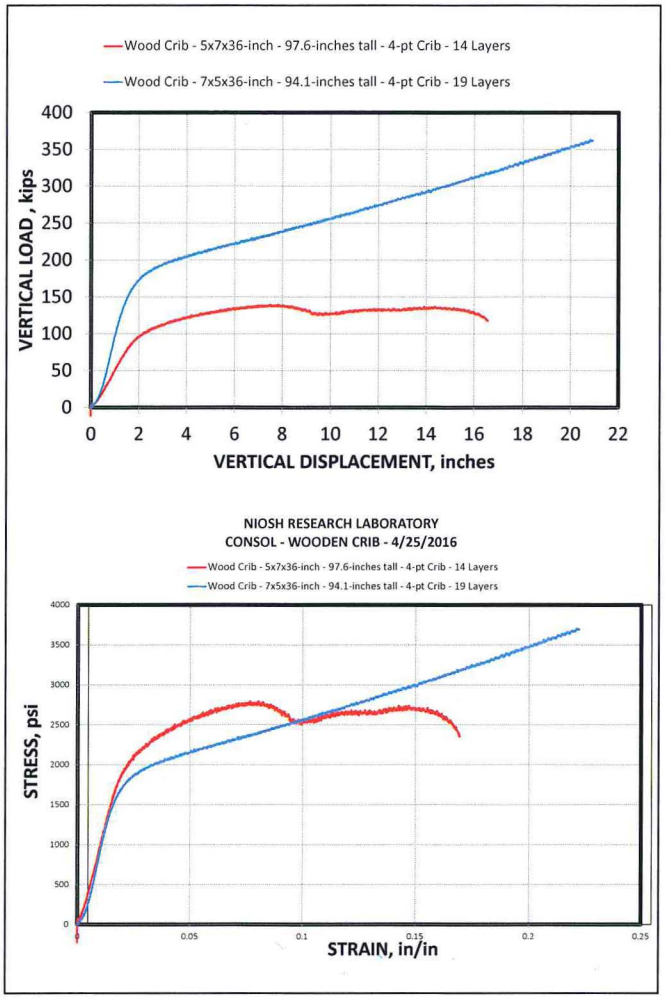

Figure 13. Load-displacement performance of a 4-point wood crib comparing the timber orientation for a 5-inch by 7-inch timber cross section.

However, in most conditions with a proper pillar design, only the abutment zone requires the additional support provided by a standing support. From that perspective, longwall tailgate support is highly inefficient. This exercise determines what length of the tailgate, beginning at the longwall face, could be supported with an equivalent coal strength if all of the standing support capacity in the tailgate were concentrated in this zone. The assumption and purpose of the exercise is that 900 psi equates to the coal strength, and, if this level of support were provided, it would be as if the entry were excavated. There would be no deformation to cause any degree of instability.

To help illustrate this hypothetical exercise, a plan view of a section of tailgate is shown in Figure 15. In this example, the tailgate entry is 20 ft wide, 12,000 ft long, and is supported with two rows of standing support on 8-ft center-to-center spacing along the entry. The supports chosen for this exercise represent five common tailgate supports: CAN, pumpable roof support, Link-N-Lock, Propsetter, and a conventional 4-point wood crib. Figure 16 shows the calculated total load resistance provided by each support system after 2 inches of convergence for the 12,000-ft-long tailgate. As seen in this figure, a wide range of support capacity is provided by the various support systems, with the pumpable support

Figure 14. Buckling of a 4-point wood crib constructed with a 5x5-inch timber contact.

providing over 4 times the capacity of the Propsetter and wood crib support systems.

Using these support capacities, the length of tailgate (see Figure 17) that could be supported with 900 psi of support resistance if all the standing support capacity were focused in this area can be calculated using Equation 3. The results are shown in Figure 18. The CAN, Link-N-Lock, and pumpable support system all provide 900-psi supported zones in excess of 200 ft. While the extent of the abutment zone depends on the depth of cover and other parameters, the zone is generally less than 200 ft in areas where the depth of cover is less than 1,000 ft. Since all of these support systems are providing adequate tailgate support at the normal installed density, it shows that, a large percentage of the time, most of the

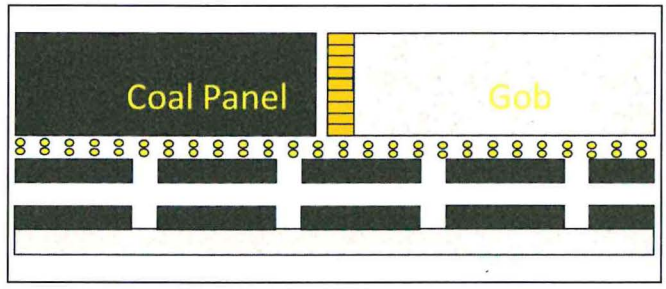

Figure 15. Illustration of a section of a tailgate entry with two rows of standing support on 8-ft center-to-center spacing.

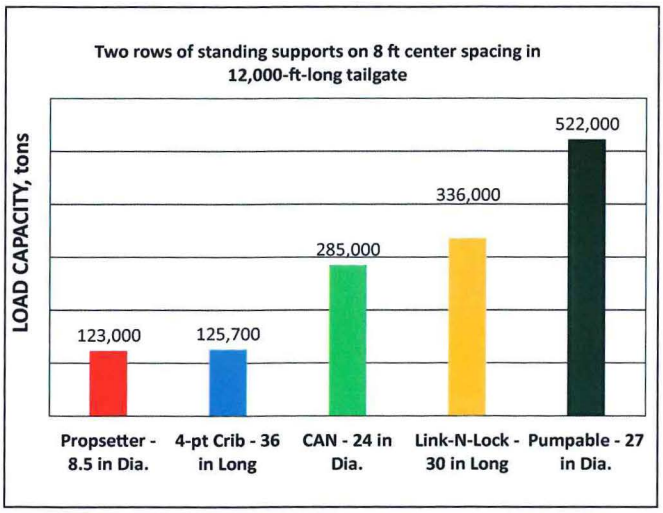

Figure 16. Total support capacity for all of standing supports for various support systems in a 12,000-ft-long tailgate.

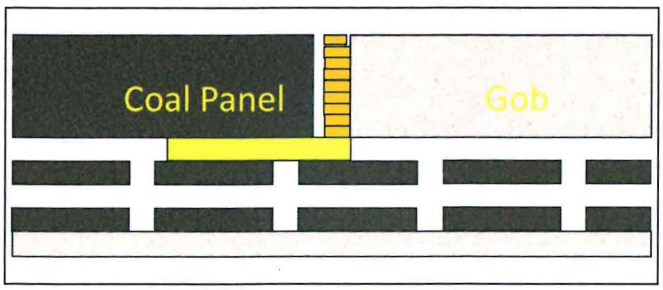

Figure 17. Illustration of a tailgate entry with the highlighted area depicting length of 900-psi equivalent standing support capacity.

support will not be used. This illustrates the inefficiency of the conventional tailgate support practice.

$$Length\ of\ 900\text{-}psi\ support = \frac{\left(\frac{Panel\ Length * Number\ of\ Rows}{Spacing(c\text{-}c)}\right) * Support\ Load}{In\text{-}situ\ Coal\ Strength * Entry\ width} \quad (3)$$

where

Length of 900-psi support = length of tailgate that could be supported with 900 psi of support resistance, ft

Panel Length = Tailgate entry length, 12,000 ft

Number of Rows = Sum of side-by-side rows of standing support, 2

Spacing (c-c) = Support spacing along tailgate entry, 8 ft

Support Load = Peak load capacity of each support, lb

In-situ Coal Strength = Compressive strength of coal, 900 psi

Entry width = Measurement from side to side of the entry, 8 ft

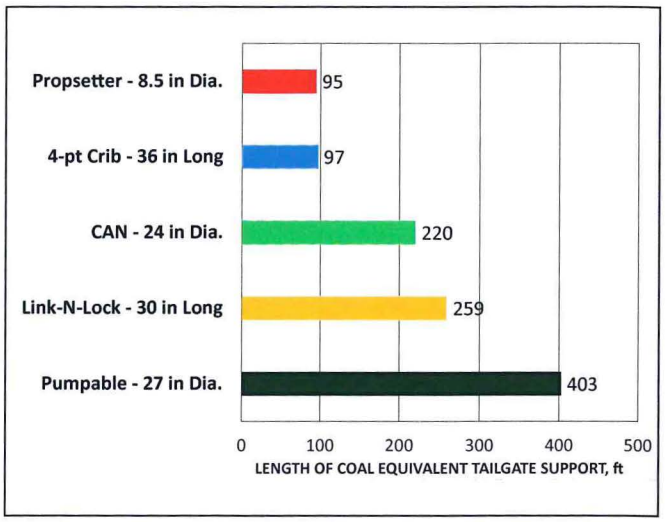

Figure 18. Length of tailgate that can be supported with 900 psi of standing support if the full capacity of the entire tailgate were concentrated in this zone.

FACTOR 10: The equivalent overburden thickness simulated by the world's largest biaxial load frame is less than you might expect.

The MRS is currently the world's largest and most powerful biaxial load frame; however, what amount of rock mass or overburden thickness does it actually simulate? The MRS lower platen is cable of applying 3 million pounds of vertical force with a usable displacement range of 0 to 24 inches vertically. Based on a rock density of 150 lb/ft^3, 50 ft of overburden rock mass exceeds the 3-million-pound capacity of this machine when acting on an area as large as the floor of the MRS (20 x 20 ft).

The MRS is the most powerful machine of its size in the world and is designed to simulate the response of the overburden rock mass on the mining entries below. A functional diagram of the load frame is shown in Figure 19. Load actuators are equipped with special hydrostatic slip bearings that permit simultaneous load and travel. The upper platen can be moved up or down and hydraulically clamped into a fixed position on the directional columns to establish a testing height up to 16 ft. Although the force capabilities of the machine are impressive, it is the ability to simulate the movement of the rock mass behavior that makes the MRS a unique and valuable tool. Maintaining ground stability has been critical to the success of coal mines in terms of both safety and productivity.

The MRS load frame was designed specifically to determine the load-displacement performance characteristics of standing support systems. Standing support systems are designed to prevent unplanned roof falls. The selection of the type of standing support is based on the interaction of the support with the surrounding rock mass, and its function is to assist the primary support system in maintaining the integrity of the immediate roof. MRS testing protocols have been developed to use the capabilities of the MRS to evaluate the strength, stiffness, and stability of standing support products.

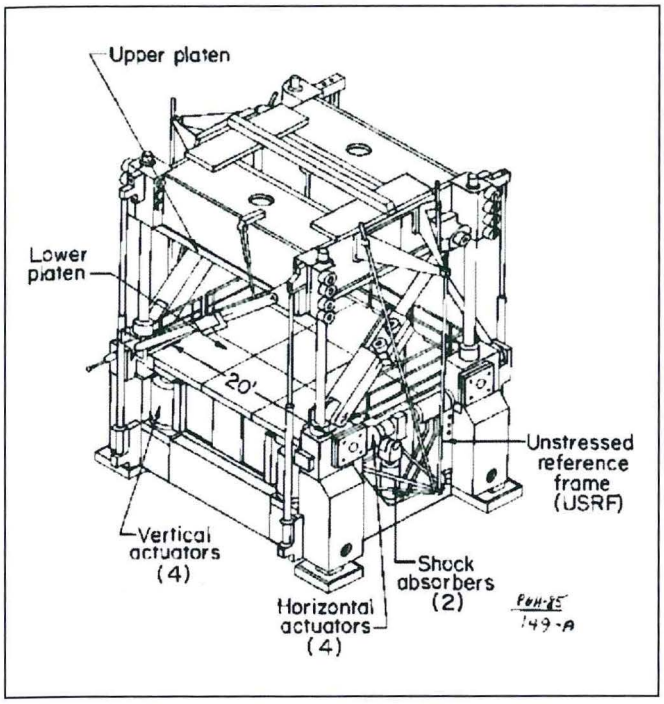

Figure 19. Functional diagram of the Mine Roof Simulator.

CONCLUSIONS

A wide variety of standing supports are used to provide additional roof support in underground coal mines. Most of these standing support systems have been used for years. Despite their widespread use, not every aspect of their performance and resulting ground support capability are always well understood. This report presents several little known factors that impact their performance. For instance, the steel shell on the outside of a CAN provides 55–65% of the rated load capacity of the CAN support, and splits in the body of the Propsetter support do not decrease rated load or yield capacity. Another example shows that construction of a 4-point wood crib from 5-inch x 6-inch x 36-inch timbers with the wide side down will provide a 44% increase in capacity compared to construction with the narrow side down at 5 inches of displacement. Knowledge of these factors helps to optimize support design and avoid misconceptions that could lead to inaccurate assessments of support performance.

DISCLAIMER

This work was conducted as part of the research program of the National Institute for Occupational Safety and Health (NIOSH). The findings and conclusions in this paper are those of the author and do not necessarily represent the views of NIOSH. Mention of company names, products, or software does not constitute endorsement by NIOSH.

REFERENCES

Barczak. T. M. and Tadolini, S. C. (2008). "Pumpable roof supports: an evolution in longwall roof support technology." *Transactions of the Society for Mining, Metallurgy, and Exploration 324*: 19–31.

Campoli, A. A. (2015). "Selection of pumpable cribs for longwall gate and bleeders entries." In: Barczak, T. M., Ed. *Proceedings of the 34th International Conference on Ground Control in Mining*. Morgantown, WV: West Virginia University, pp. 80–82.

Dolinar, D. (2010). "Ground and standing support interaction in tailgates of western U.S. longwall mines used in the development of a design methodology based on the ground reaction curve." In: Barczak, T. M., Ed. *Proceedings of the 29th International Conference on Ground Control in Mining*. Morgantown, WV: West Virginia University, pp. 152–160.

Fiscor, S, (2016). "U.S. longwall census." *Coal Age*: 20–22.

Hicks, T. (2010) *Civil Engineering Formulas*. New York, NY: McGraw Hill, pp. 416.

Zhang, P., Milam, M., Mishra, M., Hudak, W. J., and Kimutis, R. (2012). "Requirements and performance of pumpable cribs in longwall tailgate entries and bleeders." In: Barczak, T. M., Ed. *Proceedings of the 31st International Conference on Ground Control in Mining*. Morgantown, WV: West Virginia University, pp. 11.

PROCEEDINGS OF THE 36th International Conference

ON GROUND CONTROL IN MINING

Edited by

Brijes Mishra | Heather Lawson | Michael Murphy | Kyle Perry

Published by the
Society for Mining, Metallurgy & Exploration

Society for Mining, Metallurgy & Exploration (SME)
12999 E. Adam Aircraft Circle
Englewood, Colorado, USA 80112
(303) 948-4200 / (800) 763-3132
www.smenet.org

The Society for Mining, Metallurgy & Exploration (SME) is a professional society whose more than 15,000 members represents all professionals serving the minerals industry in more than 100 countries. SME members include engineers, geologists, metallurgists, educators, students and researchers. SME advances the worldwide mining and underground construction community through information exchange and professional development.

ISBN 978-0-87335-456-1